

Chain Conformations and Locations of Parts of a Block Polymer in a Lamellar Structure

Yushu Matsushita,* Katsuaki Mori,^{1a} Ryuichi Saguchi,^{1b} Ichiro Noda, and Mitsuru Nagasawa^{1c}

Department of Synthetic Chemistry, Nagoya University, Furo-cho, Chikusa-ku, Nagoya 464-01, Japan

Taihyun Chang,^{1d} Charles J. Glinka, and Charles C. Han

Materials Science and Engineering Laboratory, National Institute of Standards and Technology, Gaithersburg, Maryland 20899

Received September 12, 1989; Revised Manuscript Received March 12, 1990

ABSTRACT: The chain conformation and location of parts of a block polymer in a lamellar structure of diblock copolymers of styrene and 2-vinylpyridine were studied by small-angle neutron scattering. It was found that the chain adjacent to the junction between the two blocks is located near the boundary between domains and is contracted along the direction parallel to the lamellae to the same extent as a whole block chain with the same molecular weight, while the chain at the free end of block polymer is located in the middle of domain and is unperturbed.

Introduction

In a previous paper² we studied the chain conformation of polystyrene blocks within lamellar structures of diblock copolymers of styrene and 2-vinylpyridine with various molecular weights by small-angle neutron scattering (SANS). We reported that the block polymer is extended along the direction perpendicular to the lamellae, while it is contracted along the direction parallel to the lamellae. The extension of the block polymer is well explained by the theories of microphase-separated structures,³⁻⁷ but the contraction is not. From the molecular weight dependence of the radii of gyration of the block polymer along the parallel and perpendicular directions, we concluded that the block polymer is contracted along the parallel direction in order to keep the volume occupied by a block chain constant, when the microphase separation occurs.

Since the junction point of two blocks is located at the boundary between two domains and block polymers are deformed anisotropically in lamellar structures, the conformations of the chain near the junction point and at the free end of block polymer may be different. Moreover, mechanical properties may be affected by boundary structures or the conformation of the block chain adjacent to the junction points. In the present work, therefore, we prepared block copolymers of styrene and 2-vinylpyridine with partially deuterated polystyrene blocks and studied their location and conformation along the direction parallel to the lamellae by SANS.

Experimental Section

For this study we used three block copolymers of partially deuterated styrene and 2-vinylpyridine and the corresponding hydrogenated block copolymers, which were prepared by an anionic polymerization technique. One is a triblock copolymer of styrene-*d*₈-styrene-2-vinylpyridine, which we call the end-labeled sample, while the other two are triblock copolymers of styrene-styrene-*d*₈-2-vinylpyridine, which we call the center-labeled samples. The preparation and characterization methods have been reported previously.^{8,9} In Table I the molecular characteristics of the partially deuterated block copolymers are listed together with the corresponding hydrogenated samples. The letters D and S in the sample code denote deuterated and hydrogenated polystyrene blocks, while P denotes the poly(2-

Table I
Molecular Characteristics of Samples

blend no.	sample code	$M_n \times 10^{-3}$ ^a	M_w/M_n	Φ_s ^b
I	SDP-5	(30-17)-42	1.02	0.51
	SP-20	35-34	1.03	0.54
II	SDP-4	(152-45)-204	1.08	0.52
	SP-12	211-177	1.03	0.52
III	DSP-1	(31-97)-106	1.04	0.50
	SP-15	119-124	1.06	0.50

^a Numbers written in boldface denote the molecular weights of deuterated blocks. ^b Φ_s is the volume fraction of polystyrene determined by elemental analysis.

vinylpyridine) block. The number-averaged molecular weight of each block, M_n , is listed in the table in the same order as the letters in the corresponding sample code. As shown in the table the molecular weight distributions are narrow and the volume fraction of the styrene blocks, Φ_s , is around 0.5.

Film specimens for SANS and also for small-angle X-ray scattering (SAXS) were prepared by solvent-casting from THF solutions as described previously.¹⁰ To examine the effect of the deuterated block content to the domain scattering from microphase-separated structures in SANS,^{10,15} we prepared five film specimens with different deuterated block contents for each of the blend samples II and III in Table I. With a transmission electron microscope we observed that all the film specimens have the lamellar structure predominantly oriented in the direction parallel to the film surface.^{8,11} The predominant orientation of lamellae is also confirmed by SANS, in which the strong domain scattering was observed in the edge-view but practically no domain scattering was observed in the through-view, as will be shown in Figures 1-4 later in this paper.

Conformation measurements were carried out at room temperatures with a SANS spectrometer equipped with a two-dimensional detector at the National Institute of Standards and Technology.¹² The experimental conditions for SANS were described in detail in previous papers.^{2,10} The scattering intensities were measured with two sample orientations, that is, the edge- and through-views, where the film specimens are set perpendicular and parallel to neutron beam, respectively.²

SAXS measurements were carried out in the edge-view at room temperatures with a Kratky U-slit camera of the Anton Paar Co. to compare the diffraction patterns in SAXS with those in SANS from the same film specimens. The scattering volume in SAXS was much smaller than that in SANS, as the incident beam sizes were ca. 10 mm × 0.1 mm in SAXS and ca. 15 mm ϕ in SANS.

Since a slit collimation system was used in the SAXS measurements, the desmearing of data was carried out according to Glatzer's program¹³ to yield the corrected scattering intensity for finite slit width and length. The experimental conditions were the same as those reported previously.^{10,11}

Results and Discussion

A. Location of Parts of a Block Chain in a Lamellar Structure. Figures 1a and 2a show the SANS and SAXS data in the edge-view for blend samples II (center-labeled sample) and III (end-labeled sample), respectively. The SANS intensity was obtained by averaging the data within the sector of $\pm 5^\circ$ around 0° of the azimuthal angle on the detector. The SAXS intensity was used without desmearing, since the diffraction peaks in the desmeared data appear at the same scattering angle as the smeared ones within experimental errors. The SANS and SAXS data of blend sample I (center-labeled sample) are similar to those in Figure 1a, so they are not shown here. In these figures additional diffraction peaks of domain scattering are observed in SANS in comparison with those in SAXS, though the first-order diffraction peaks of SAXS data in Figure 1a and of SANS data in Figure 2a cannot be observed clearly, because these peaks arise near the limit of the low-angle resolution of the apparatuses. The appearance of the new peaks suggests the localization of the deuterated parts in a particular location in a polystyrene domain.

If we assume that the deuterated parts of the center-labeled sample are localized near the boundary between the two domains in the blend samples I and II, the profiles of electron and scattering length densities, which are the contrast factors in SAXS and SANS, respectively, are given as schematically shown in Figure 1b. As shown in the figure, the difference between scattering lengths of hydrogenated polystyrene and poly(2-vinylpyridine) is much smaller than that between scattering lengths of deuterated polystyrene and poly(2-vinylpyridine), while there is no effective difference in electron density between deuterated and hydrogenated polystyrenes. The diffraction patterns in both SAXS and SANS in Figure 1a can be well explained by these contrast profiles. In this figure the diffraction peaks of both odd- and even-number orders are observed in SANS, while only the odd-number orders are observed in SAXS, because the width of the region with the higher scattering length density is much narrower than that of the region with the lower scattering length density in the contrast profiles for SANS, while both widths are almost the same in the contrast profiles for SAXS as shown in Figure 1b.^{11,14} Moreover, the diffraction peaks in SANS appear at q values about twice as large as those in SAXS, because the distance between repeating units in the scattering length density profile is practically half of that in the electron density profile.

In the case of the blend sample III with the end-labeled block, we can also explain both scattering patterns in Figure 2a, if we assume that the deuterated part at the free end of the polystyrene block is located in the middle of the polystyrene domain as shown in Figure 2b. The appearance of diffraction peaks of both odd- and even-number orders in SANS is due to the same reason mentioned above. The peaks of odd-number orders in SANS appear at the same values of q as those in SAXS, because the distance between repeating units in electron density and scattering length density should be equal as shown in Figure 2b.

B. Conformation of Parts of a Block Chain in a Lamellar Structure. Because of the localization of the partially deuterated blocks in the polystyrene domains

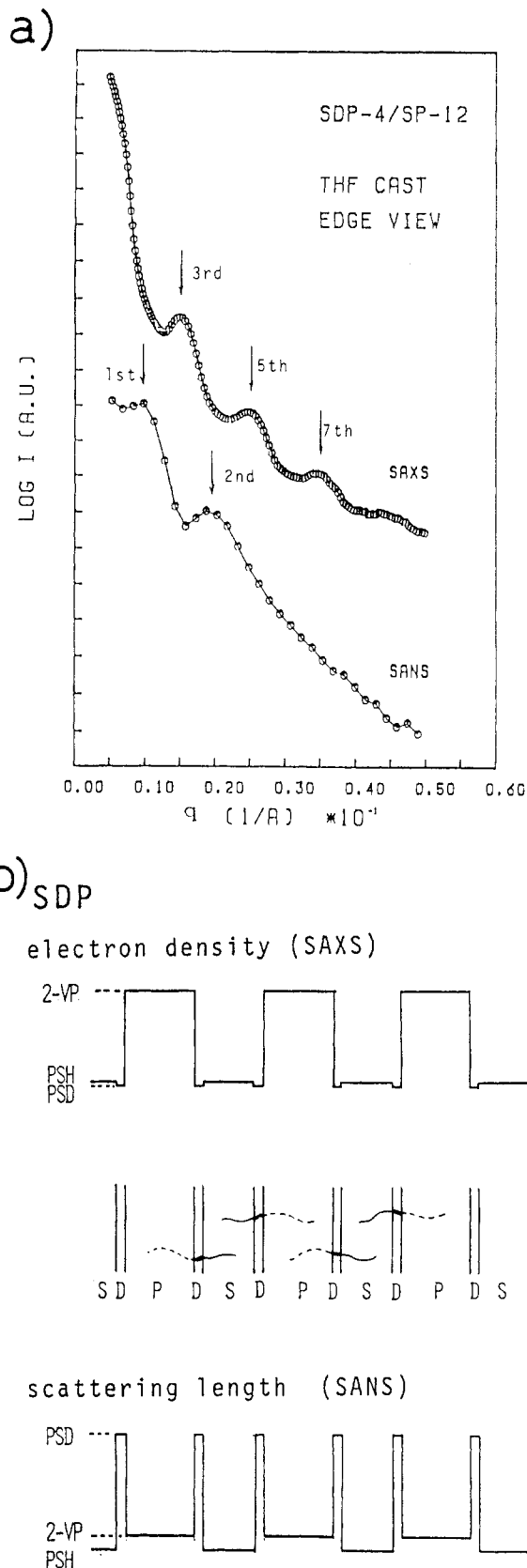
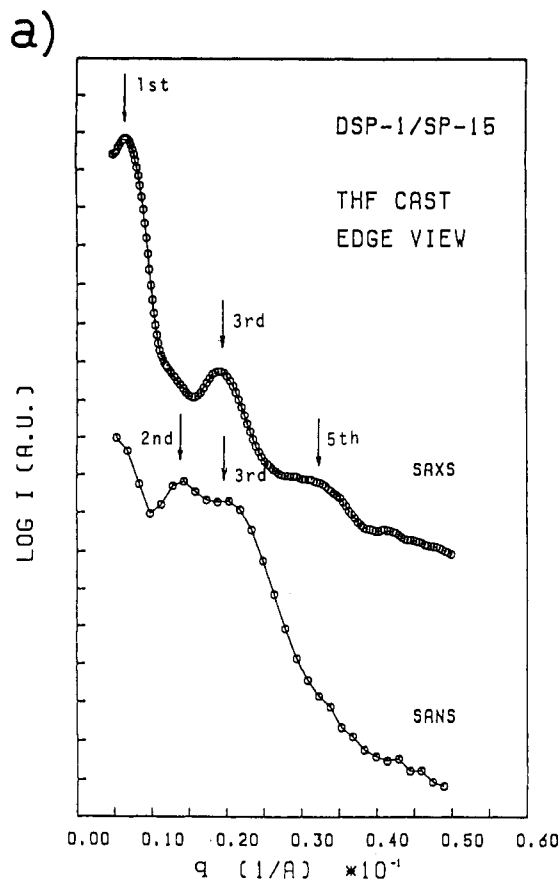


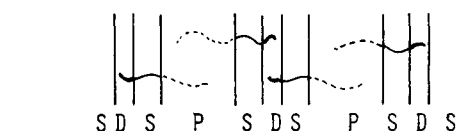
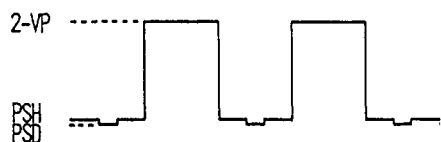
Figure 1. (a) Comparison between SAXS and SANS data in the edge-view for blend sample II (SDP-4/SP-12) at the mixing ratio of 50/50 by weight. (b) Schematic representation of the location of deuterated chain within a microdomain and the corresponding profiles of electron density and scattering length density.

mentioned above, we cannot eliminate the domain scattering in the edge-view, even if the average scattering length density of the polystyrene domain is equal to the scattering length density of the poly(2-vinylpyridine)



b) DSP

electron density (SAXS)



scattering length (SANS)

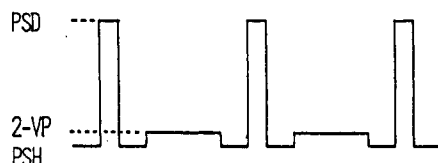


Figure 2. (a) Comparison between SAXS and SANS data in the edge-views for the blend sample III (DSP-1/SP-15) at the mixing ratio of 33/67 by weight. (b) Schematic representation of the location of the deuterated chain within a microdomain and the corresponding profiles of electron density and scattering length density.

domain. The details will be reported elsewhere.¹⁵ In general, two kinds of contrast matching, such as phase and composition matching, are needed to eliminate the domain scattering from microphase-separated structures containing

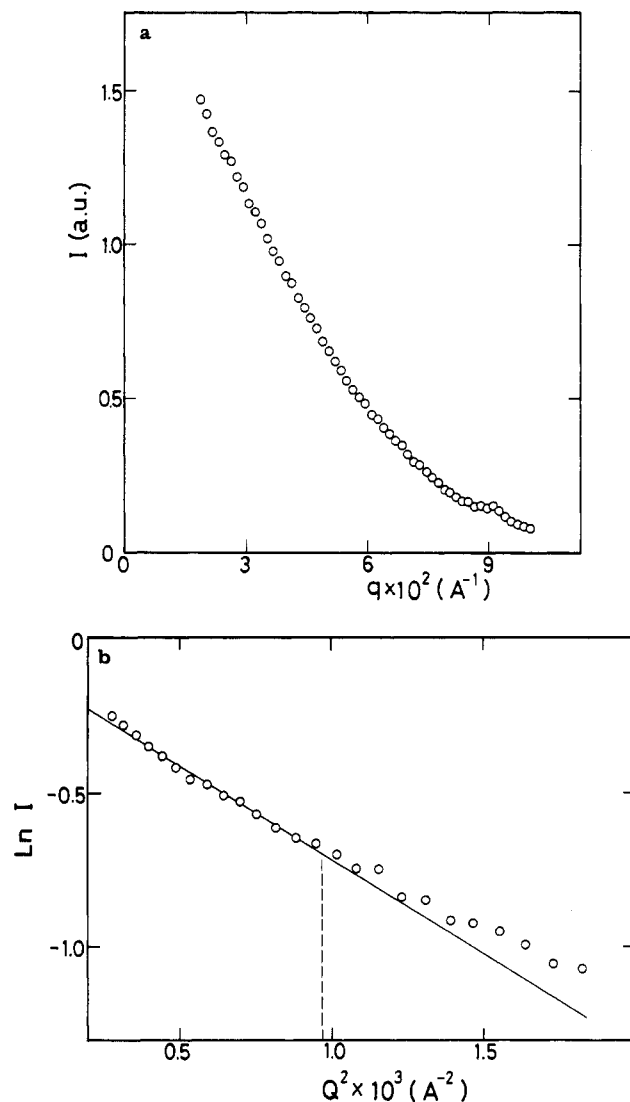


Figure 3. (a) Single-chain scattering in the through-view for the blend sample I (SDP-5/SP-20) at the mixing ratio of 25/75 by weight. (b) Guinier plot of the data in Figure 3a. The broken line denotes the upper limit of the Guinier range.

partially deuterated block copolymers.¹⁶ Moreover, the chain lengths of deuterated and hydrogenated parts should be matched to extract the single-chain scattering. However, if the domain where the deuterated parts are located can be regarded as a new lamella, at least for SANS, and also if the lamella is highly oriented parallel to the film surface, the domain scattering does not arise in the through-view.² This is the case for the present film specimens. Since the chain lengths of deuterated and hydrogenated blocks must be equal in the lamellarlike domain, where the deuterated segments are located, moreover, we can observe the single-chain scattering of a part of a block chain in the through-view. Figures 3a and 4a show the single-chain scatterings from blend sample I (center-labeled sample) and blend sample III (end-labeled sample) in the through-view, respectively, where their intensities were circularly averaged.

The radius of gyration of a part of a block polymer chain along the k axis, $R_{g,k}$, is evaluated by the Guinier equation

$$I(q) = I(0) \exp(-q^2 R_{g,k}^2) \quad (1)$$

where $q = (4\pi/\lambda) \sin \theta$ and 2θ is the scattering angle. If we define the direction perpendicular to the lamella as the y direction, the x and z directions are equivalent in the Cartesian coordinate. Hence, we call the dimension

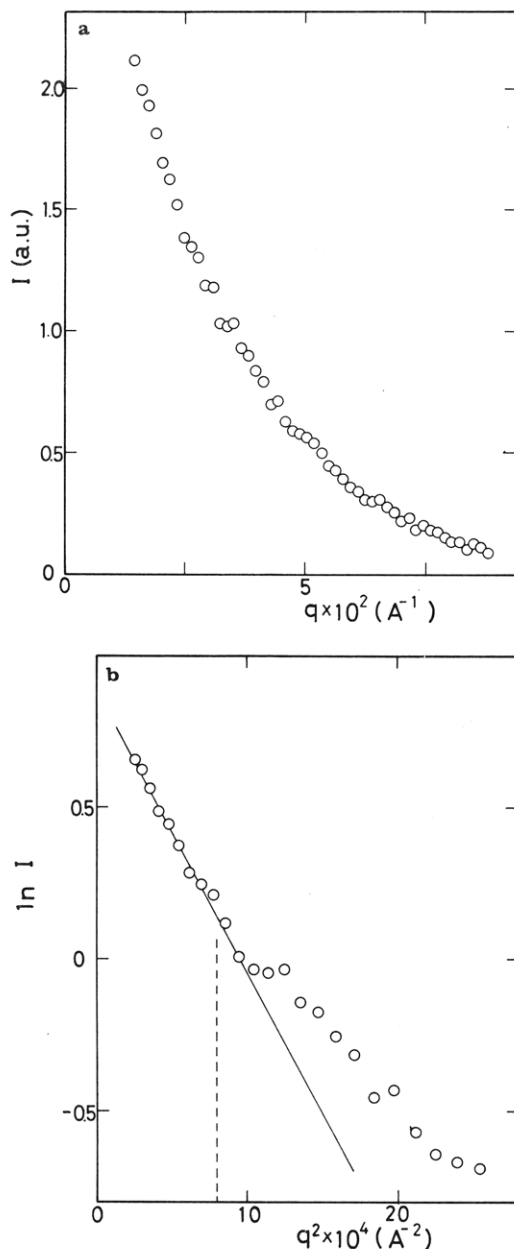


Figure 4. (a) Single-chain scattering in the through-view for blend sample III (DSP-1/SP-15) at the mixing ratio of 33/67 by weight. (b) Guinier plot of the data in Figure 4a. The broken line denotes the upper limit of the Guinier range.

Table II
Chain Dimensions of Parts of Block Chains

blend no.	$M(D) \times 10^{-3}$	$R_{g,x}, \text{\AA}$	$R_{g,x}/R_{g,x0}$	$\langle \cos^2 \phi \rangle^{1/2}$
I	17	17.8 ± 0.5	0.87 ± 0.03	0.96
II	45	29.7 ± 0.7	0.88 ± 0.03	0.94
III	31	27.2 ± 1.2	0.98 ± 0.04	0.96

obtained from the through-view measurements the radius of gyration of the portion of the block polymer along the x axis, $R_{g,x}$, for convenience.² Figures 3b and 4b show the Guinier plots of the data in Figures 3a and 4a, respectively. The $R_{g,x}$ values were evaluated from the initial slope of the Guinier plot in the Guinier range for a sphere with the same radius of gyration, i.e., $q^2 R_{g,x}^2 < 1.3^2/3$, as described in a previous paper.² The $R_{g,x}$ values thus obtained and their ratios to the unperturbed radii of gyration are listed in Table II. The unperturbed radius of gyration of deu-

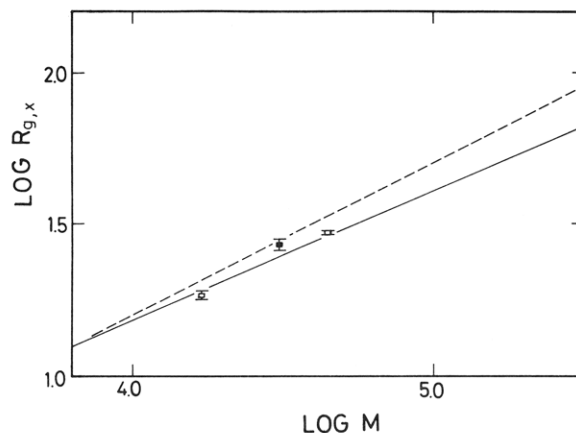


Figure 5. Double-logarithmic plots of the radius of gyration along the x axis vs molecular weight for the chains adjacent to the junction point (□) and at the free end (■) of block polymers. The solid and broken lines denote eqs 3 and 2, respectively.

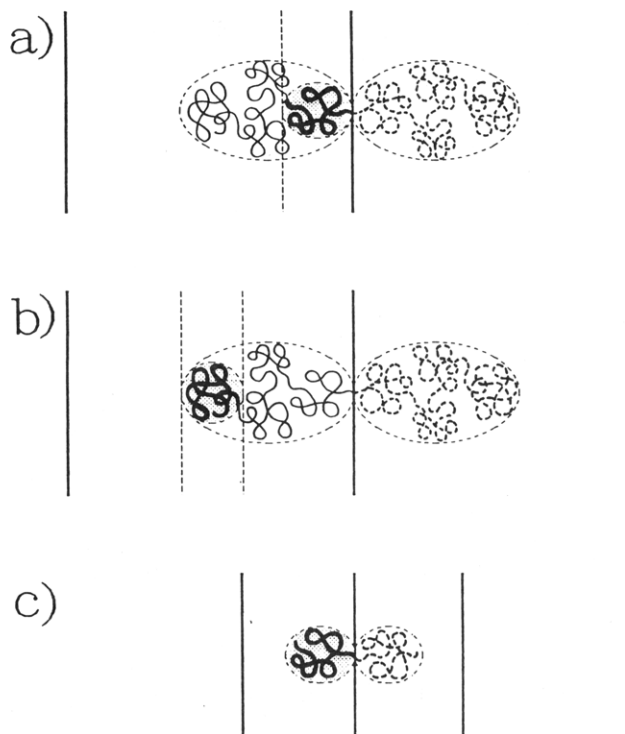


Figure 6. Schematic drawing of the chain conformations of parts of block chains in comparison with that of a whole block chain in lamellae from the edge-view: (a) a part of a chain adjacent to the junction point; (b) a part of a chain at the free end; (c) a whole block chain with the same molecular weight as that of the parts (a and b) of a block polymer.

terated polystyrene along any axis was evaluated by¹⁷

$$R_{g,k0} = 0.159M^{0.5} \quad 2.1 \times 10^4 < M < 1.1 \times 10^6 \quad (2)$$

The errors in the $R_{g,x}$ values for blend samples II and III were estimated by taking into account both the standard deviation of the slope in the linear least-squares fit of the Guinier plots and the deviation of the observed radius of gyration for each of the film specimens with different deuterated block contents as mentioned before, from the average value, and the error for blend sample I was estimated from the standard deviation in the Guinier plot, of which the data were obtained in a measuring time about twice as long as that in the data for blend samples II and III. Figure 5 shows double-logarithmic plots of the $R_{g,x}$ values vs the number-averaged molecular weight, M_n , of deuterated parts for the center- and end-labeled samples.

The broken and solid lines denote eq 2 and the following experimental relationship between $R_{g,x}$ and M for the whole polystyrene blocks in lamellae,² respectively.

$$R_{g,x} = 0.28_g M^{0.43} \quad 2.1 \times 10^4 < M < 1.62 \times 10^5 \quad (3)$$

It is apparent in Table II and Figure 5 that the chains near the junction points between the two block polymers in blend samples I and II are contracted along the x axis, i.e., the direction parallel to the lamellae, to the same extent as those of the whole block polymers with the same molecular weights,² while the chain at the free end of the block in blend sample III is unperturbed. The conformations of portions of the block chains in lamellar microdomains are compared schematically with that of a whole block polymer in Figure 6.

In the above discussion we assumed that the lamellae that contain deuterated chains are perfectly oriented along the direction parallel to the film surface. Actually, however, the orientation cannot be expected to be perfect, as mentioned previously.² Experimentally, the degree of orientation can be estimated from the scattering data in the edge-view. The details of the evaluation method were reported previously.² The last column in Table II shows $\langle \cos^2 \phi \rangle^{1/2}$, where ϕ is the azimuthal angle on the detector, i.e., the mean-square root of the orientation angle of the lamella, which is around 0.95. This means that the lamellae are almost perfectly oriented. Therefore, the above conclusions still hold, though quantitative modifications are necessary.

In summary, the chain adjacent to the junction between two blocks is located near the boundary between domains and is contracted along the direction parallel to the lamellae to the same extent as the whole block polymer with the same molecular weight. On the other hand, the chain at the free end of a block polymer is located in the middle of a domain and is unperturbed.

Acknowledgment. We thank the Japan Society for Promotion of Science and the National Science Foundation under the Japan-U.S. Cooperative Science Program for partial support.

References and Notes

- (1) Present address: (a) Tosoh Corp., Kasumi 1-8, Yokkaichi, Mie 510, Japan. (b) Shin-Etsu Chemical Industry Co., Ltd., Jyoetsu, Niigata 942, Japan. (c) Toyota Technological Institute, 2-12-1 Hisakata, Tenpaku-ku, Nagoya 469, Japan.
- (2) Matsushita, Y.; Mori, K.; Mogi, Y.; Saguchi, R.; Noda, I.; Nagasawa, M.; Chang, T.; Glinka, C. J.; Han, C. C. *Macromolecules*, in press.
- (3) Meier, D. J. *J. Polym. Sci., Part C* **1969**, *26*, 81. Meier, D. J. *Block and Graft Copolymers*; Burke, J. J., Weiss, V., Eds.; Syracuse University Press: Syracuse, NY, 1973.
- (4) (a) Helfand, E. *Macromolecules* **1975**, *8*, 522. (b) Helfand, E.; Wasserman, Z. R. *Macromolecules* **1976**, *9*, 879.
- (5) Semenov, A. V. *Sov. Phys.-JETP (Engl. Transl.)* **1985**, *61* (4), 733.
- (6) (a) Ohta, T.; Kawasaki, K. *Macromolecules* **1986**, *19*, 2621. (b) Kawasaki, K.; Ohta, T.; Kohrogui, M. *Macromolecules* **1988**, *21*, 2972.
- (7) Kawasaki, K.; Kawakatsu, T., accepted for publication in *Macromolecules*.
- (8) Matsushita, Y.; Nakao, Y.; Saguchi, R.; Choshi, H.; Nagasawa, M. *Polym. J.* **1986**, *18*, 493.
- (9) Matsushita, Y.; Nakao, Y.; Shimizu, K.; Noda, I.; Nagasawa, M. *Macromolecules* **1988**, *21*, 2780.
- (10) Matsushita, Y.; Nakao, Y.; Saguchi, R.; Mori, K.; Choshi, H.; Muroga, Y.; Noda, I.; Nagasawa, M.; Chang, T.; Glinka, C. J.; Han, C. C. *Macromolecules* **1988**, *21*, 1802.
- (11) Matsushita, Y.; Mori, K.; Saguchi, R.; Nakao, Y.; Noda, I.; Nagasawa, M. *Macromolecules*, in press.
- (12) Glinka, C. J.; Rowe, J. M.; LaRock, J. G. *J. Appl. Cryst.* **1986**, *19*, 427.
- (13) Glatter, O. *J. Appl. Cryst.* **1974**, *7*, 147.
- (14) Hasegawa, H.; Hashimoto, T.; Kawai, H.; Lodge, T. P.; Amis, E. J.; Han, C. C. *Macromolecules* **1985**, *18*, 67.
- (15) Matsushita, Y.; Mori, K.; Saguchi, R.; Noda, I.; Nagasawa, M.; Han, C. C., in preparation.
- (16) Quan, X.; Koberstein, J. T. *J. Polym. Sci., Part B: Polym. Phys.* **1987**, *25*, 1381.
- (17) Cotton, J. P.; Decker, D.; Benoit, H.; Farnoux, B.; Higgins, J.; Jannink, G.; Ober, R.; Picot, C.; des Cloizeaux, J. *Macromolecules* **1974**, *6*, 863.